

Raised Step-Up Converter Using Three-Winding Coupled Inductor for Fuel Cell Potential Source Purposes

K. Jahnavi

M tech in Power Electronics
Prasad Engineering College

S. Sahithi

Associate Professor & Head of Dept EEE
Prasad Engineering College

Abstract

Abstract: This paper presents a high step-up converter for fuel cell energy source applications. The proposed high step-up dc-dc converter is devised for boosting the voltage generated from fuel cell to be a 400-V dc-bus voltage. Through the three-winding coupled inductor and voltage doubler circuit, the proposed converter achieve high step-up voltage gain without large duty cycle. The passive lossless clamped technology not only recycles leakage energy to improve efficiency but also alleviates large voltage spike to limit the voltage stress. Finally, the fuel cell as input voltage source 60–90 V integrated into a 2-kW prototype converter was implemented for performance verification. Under output voltage 400-V operation, the highest efficiency is up to 96.81%, and the full-load efficiency is 91.32%.

Index Terms: Coupled inductor, fuel cell energy source applications, high step-up converter.

1. INTRODUCTION

Recently, the cost increase of fossil fuel and new regulations of CO₂ emissions have strongly increased the interests in renewable energy sources. Hence, renewable energy sources such as fuel cells, solar energy, and wind power have been widely valued and employed. Fuel cells have been considered as an excellent candidate to replace the conventional diesel/gasoline in vehicles and emergency power sources. Fuel cells can provide clean energy to users without CO₂ emissions. Due to stable operation with high-efficiency and sustainable/renewable fuel supply, fuel cell has been increasingly accepted as a competently alternative source for the future. The excellent features such as small size and high conversion efficiency make them valuable and potential. Hence, the fuel cell is suitable as power supplies for energy source applications. Generally speaking, a typical fuel cell power supply system containing a high step-up converter is shown in Fig. 1.

The generated voltage of the fuel cell stack is rather low. Hence, a high step-up converter is strongly required to lift the voltage for applications such as dc micro grid, inverter, or battery.

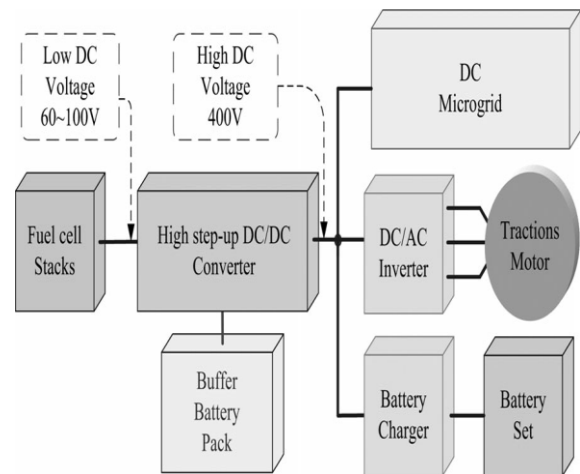


Fig. 1. Fuel cell power supply system with high step-up converter.

Ideally, a conventional boost converter is able to achieve high step-up voltage gain with an extreme duty cycle. In practice, the step-up voltage gain is limited by effects of the power switch, rectifier diode, and the resistances of the inductors and capacitors. In addition, the extreme duty cycle may result in a serious reverse-recovery problem and conduction losses. A flyback converter is able to achieve high step-up voltage gain by adjusting the turns ratio of the transformer winding [17], [18]. However, a large voltage spike leakage energy causes may destroy the main switch. In order to protect the switch devices and constrain the voltage spike, a high-voltage-rated switch with high on-state resistance (*R_{DS-ON}*) and a snubber circuit are usually adopted in the flyback converter, but the leakage energy still be consumed. These methods will diminish the power conversion efficiency [19]–[21]. In order to increase the conversion efficiency and voltage gain, many technologies such as zero-voltage switching (ZVS), zero-current switching (ZCS), coupled

inductor, active clamp, etc. [22]–[24] have been investigated. Some high step-up voltage gain can be achieved by using switched-capacitor and voltage-lift techniques [25]–[28], although switches will suffer high current and conduction losses. In recent years, coupled-inductor technology with performance of leakage energy recycle is developed for adjustable voltage gain; thus, many high step-up converters with the characteristics of high voltage gain, high efficiency, and low voltage stress have been presented [29]–[39]. In addition, some novel high step-up converters with three-winding coupled inductor have also been proposed, which possess more flexible adjustment of voltage conversion ratio and voltage stress [37], [39]. In this paper, the proposed high step-up converter designed for fuel cell energy source applications is shown in Fig. 2.

The fuel cell with inertia characteristics as main power source cannot respond to load dynamics well. Therefore, lithium iron phosphate can be an excellent candidate for secondary source to react to fast dynamics and contribute to load peaking. The proposed converter with fuel cell input source is suitable to operate in continuous conduction mode (CCM) because the discontinuous conduction mode operation results in large input current ripple and high peak current, which make the fuel cell stacks difficult to afford.

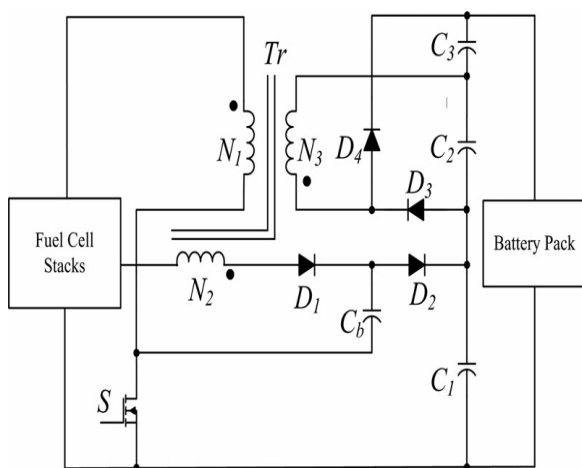


Fig. 2. Proposed high step-up converter

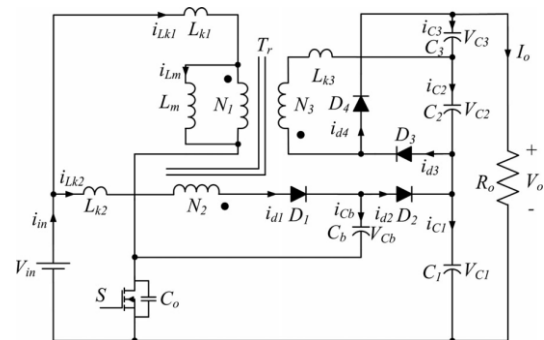


Fig. 3. Equivalent circuit of the proposed converter.

2. OPERATING PRINCIPLE OF THE PROPOSED CONVERTER

The proposed converter employs a switched capacitor and a voltage-doubler circuit for high step-up conversion ratio. The switched capacitor supplies an extra step-up performance; the voltage-doubler circuit lifts of the output voltage by increasing the turns ratio of coupled-inductor. The advantages of proposed converter are as follows:

- 1) Through adjusting the turns ratio of coupled inductor, the proposed converter achieves high step-up gain that renewable energy systems require;
- 2) Leakage energy is recycled to the output terminal, which improves the efficiency and alleviates large voltage spikes across the main switch;
- 3) Due to the passive lossless clamped performance, the voltage stress across main switch is substantially lower than the output voltage;
- 4) Low cost and high efficiency are achieved by adopting low-voltage-rated power switch with low RDS-ON;
- 5) By using three-winding coupled inductor, the proposed converter possesses more flexible adjustment of voltage conversion ratio and voltage stress on each diode.

The equivalent circuit of the proposed converter shown in Fig. 3 is composed of a coupled inductor Tr , a main power switch S , diodes $D1, D2, D3$, and $D4$, the switched capacitor Cb , and the output filter capacitors $C1, C2$, and $C3$. Lm is the magnetizing inductor and $Lk1, Lk2$, and $Lk3$ represent the leakage inductors. The turns ratio of coupled inductor $n2$ is equal to $N2/N1$,

and n_3 is equal to N_3/N_1 , where N_1, N_2 , and N_3 are the winding turns of coupled inductor.

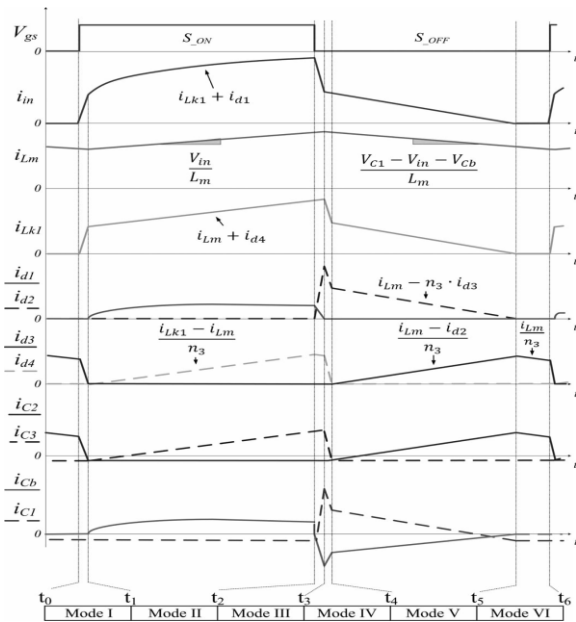


Fig. 4. Steady-state waveforms in CCM operation.

The steady-state waveforms of the proposed converter operating in CCM are depicted in Fig. 4

3. STEADY-STATE ANALYSIS

In order to simplify the CCM steady-state analysis, the following factors are taken into account. All the leakage inductors of the coupled inductor are neglected, and all of components are ideal without any parasitic components. The voltages V_b , V_{C1} , V_{C2} , and V_{C3} are considered to be constant due to infinitely large capacitances.

A. Step-Up Gain

During the turn-on period of switch S , the following equations can be written as:

$$V_{C3} = V_{N3} = n_3 \cdot V_{in} \quad (1)$$

$$V_{Cb} = V_{in} + V_{N2} = (n_2 + 1) \cdot V_{in}. \quad (2)$$

During the turn-off period of switch S , the following equations can be expressed as:

$$V_{C2} = n_3 [V_{C1} - (2 + n_2) \cdot V_{in}] \quad (3)$$

$$V_{C1} = \left(\frac{D}{1-D} + 2 + n_2 \right) \cdot V_{in}. \quad (4)$$

Thus, the output voltage V_O can be expressed as

$$V_O = V_{C1} + V_{C2} + V_{C3}. \quad (5)$$

By substituting (1), (3), and (4) into (5), the voltage gain of the proposed converter is given by

$$M_{CCM} = \frac{V_o}{V_{in}} = n_2 + \frac{2-D+n_3}{1-D}. \quad (6)$$

Equation (6) shows that high step-up gain can be easily obtained by increasing the turns ratio of the coupled inductor without large duty cycle.

The step-up gain versus duty ratio under various turns ratios is plotted in Fig. 6.

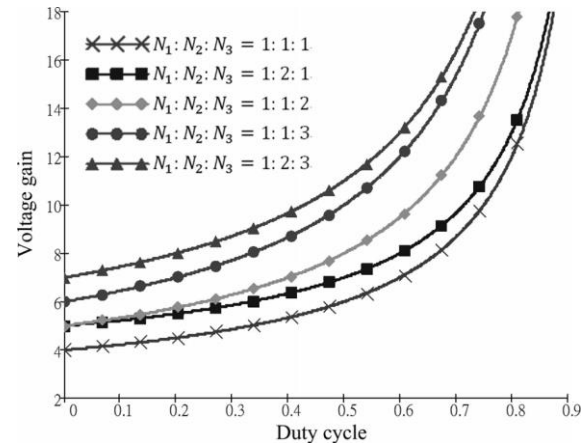


Fig. 6. Step-up gain versus duty ratio under various turns ratios.

B. Voltage Stress

The voltage stress on the main switch is given as follows:

$$M_S = \frac{V_{S1}}{V_{out}} = \frac{1}{2-D+(1-D)n_2+n_3}. \quad (7)$$

When the switching S is turned OFF, the diodes $D1$ and $D3$ are reverse biased. Therefore, the voltage stresses of $D1$ and $D3$ are as follows:

$$M_{D1} = \frac{V_{D1}}{V_{out}} = \frac{1 + n_2}{2 - D + (1 - D)n_2 + n_3} \quad (8)$$

$$M_{D4} = \frac{V_{D3}}{V_{out}} = \frac{n_3}{2 - D + (1 - D)n_2 + n_3} \quad (9)$$

When the switch S is in turn-on period and the diodes $D2$ and $D3$ are reverse biased. Therefore, the voltage stresses of diodes $D2$ and $D3$ are as follows:

$$M_{D2} = \frac{V_{D2}}{V_{out}} = \frac{1}{2 - D + (1 - D)n_2 + n_3} \quad (10)$$

$$M_{D3} = \frac{V_{D4}}{V_{out}} = \frac{n_3}{2 - D + (1 - D)n_2 + n_3} \quad (11)$$

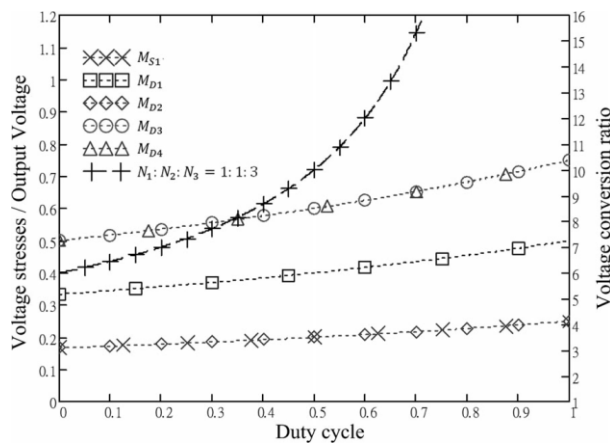


Fig. 7. Voltage stresses on the main switch and diodes.

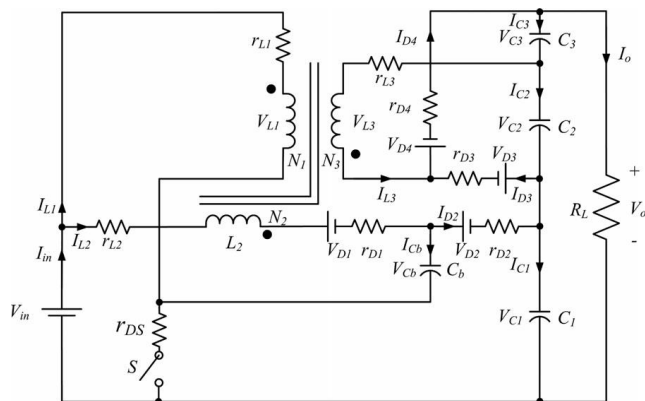


Fig. 8. Equivalent circuit including inductor conduction losses.

Equations (7)–(11) can be illustrated to determine the maximum voltage stress on each power drives. The voltage stress on the switch and diodes is plotted in Fig. 7.

C. Analysis of Conduction Losses

Some conduction losses are caused by resistances of semiconductor components and coupled inductor. Thus, all the components in the analysis of conduction losses are not continuously assumed to be ideal, except for all the capacitors. Diode reverse recovery problems, core losses, switching losses, and the ESR of capacitors are not discussed in this section. The characteristics of leakage inductor are disregarded because of energy recycling. The equivalent circuit, which includes the conduction losses of coupled inductors and semiconductor components, is shown in Fig. 8. The corresponding equivalent circuit includes copper resistances r_{L1} , r_{L2} , and r_{L3} , all the diode forward resistances r_{D1} , r_{D2} , r_{D3} , and r_{D4} , and the on-state resistance R_{DS-ON} of the power switch.

Small-ripple approximation was used to calculate conduction losses and all currents that pass through components were approximated by the dc components. Thus, the magnetizing current and capacitor voltages are assumed to be constant. Finally, through voltage-second balance and capacitor-charge balance, the voltage conversion ratio with conduction losses can be derived from

$$\frac{V_o}{V_{in}} = \frac{(n_2 + \frac{2-D+n_3}{1-D}) - K}{1 + \frac{\alpha}{R_L(1-D)^2} + \frac{r_{L3}}{R_L D(1-D)} + \frac{\beta}{R_L(1-D)} + \frac{\gamma}{R_L D}} \quad (12)$$

where

$$\begin{cases} K = \frac{V_{D1} + V_{D2} + V_{D3} + V_{D4}}{V_{in}} \\ \alpha = (1 + n_2) D \cdot r_{L1} + (1 + n_3) D \cdot r_{DS} \\ \beta = (1 + 2n_2 + n_3) r_{L1} + r_{L3} + r_{D2} + r_{D3} \\ \quad + (2 + n_2 + 2n_3) r_{DS} \\ \gamma = r_{L2} + r_{D1} + r_{D4} + (1 + n_2 + n_3) r_{DS} \end{cases}$$

Efficiency is expressed as follows:

$$\eta = \frac{V_{in} - n_2 + \frac{2-D+n_3}{1-D} \cdot (V_{D1} + V_{D2} + V_{D3} + V_{D4})}{V_{in} + \frac{\alpha}{R_L(1-D)^2} + \frac{r_{L3}}{R_L D(1-D)} + \frac{\beta}{R_L(1-D)} + \frac{\gamma}{R_L D}} \quad (13)$$

4. DESIGN AND EXPERIMENTS OF THE PROPOSED CONVERTER

Design Guidelines

The PEMFC module consists of fuel cell stack of the PEM type, mechanical auxiliaries, and electronic control module. During normal operation, the generated voltage of fuel cell is related to load. Under full-load operation, the rated power is 2 kW and the corresponding voltage is 60 V, which is shown in Fig. 10. Also, the nominal parameter is shown in Table II. The proposed high step-up converter is initially designed to convert the generated dc voltage from fuel cell stacks into 400 V. The required step-up conversion ratio is up to 6.7. Therefore, in order to make the duty cycle lower than 0.5 to decrease the conduction losses, the key design step is to determine the turns ratio of the coupled inductor. The relationship of duty cycle versus conversion efficiency and voltage gain under different turns ratios is shown in Fig. 11. Thus, the turns ratio of the coupled inductor is set as 1:1:1.5. The magnetizing inductor can be designed based on the current ripple percentage of magnetizing inductor under full-load operation, and the related equations are given as

$$I_{Lm} = \frac{1 + n_3}{1 - D_{max}} I_{o,max} \quad (14)$$

$$L_m = \frac{V_{in,min} \times D_{max}}{f \times 2\Delta i_{Lm}} \quad (15)$$

The capacitors can be designed based on the voltage ripple percentage of capacitor under full-load operation, and the related equations are given as

$$C_1 = C_3 = \frac{I_{o,max} \times D_{max}}{f \times \Delta v_C} \quad (16)$$

$$C_b = C_2 = \frac{I_{o,max}}{f \times \Delta v_C} \quad (17)$$

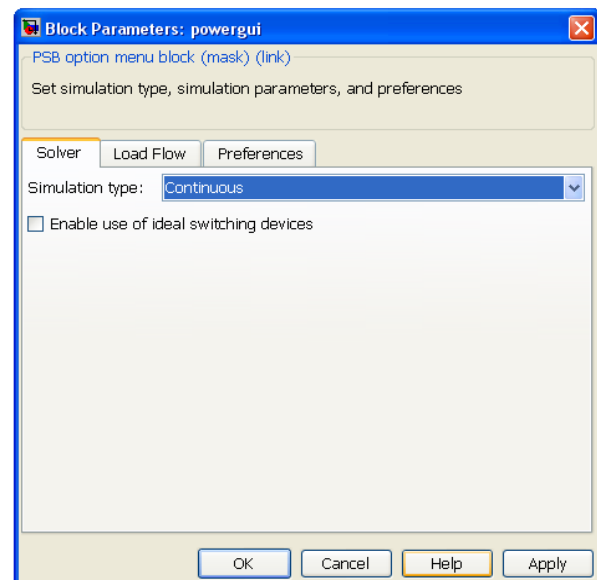
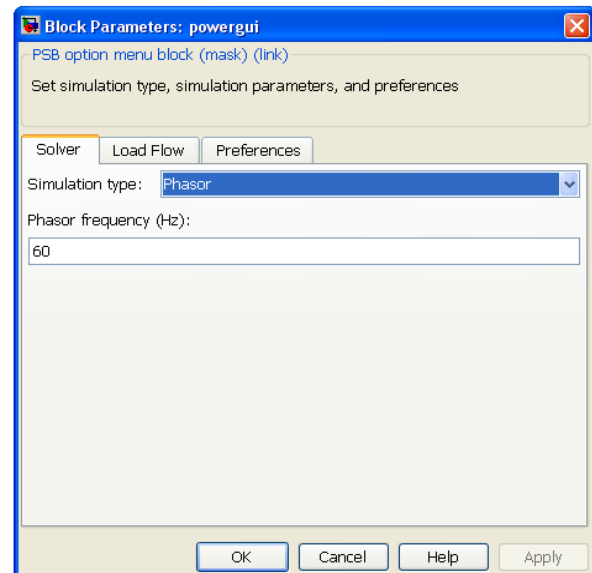
5. Simulation Results

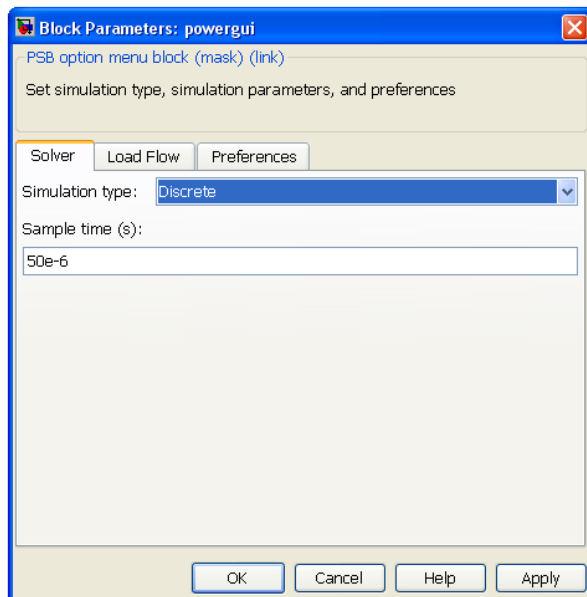
To specify the simulation type, parameters, and preferences, select Configure parameters in the Powergui dialog. This opens another dialog box with the Powergui block parameters. This dialog box contains the following tabs:

- Solver Tab
- Load Flow Tab
- Preferences Tab

Solver Tab

The configuration of the Solver tab depends on the option selected from the Simulation type drop-down list.





Simulation type

- Select Continuous to perform a continuous solution of the model.
- Select Discrete to perform a discretization of the model. The sample time is specified by the Sample time parameter.
- Select Phasor to perform phasor simulation of the model, at the frequency specified by the Phasor frequency parameter.

6. CONCLUSION

In this paper, a high step-up dc–dc converter for fuel cell hybrid electric vehicle applications is clearly analyzed and successfully verified. By using technologies of three-winding coupled inductor, switched capacitor, and voltage doubler circuit, the high step-up conversion can be efficiently obtained. The leakage energy is recycled and large voltage spike is alleviated; thus, the voltage stress is limited and the efficiency is improved. The full-load efficiency is up to 91.32% and the maximum efficiency is up to 96.81%. The voltage stress on the main switch is clamped as 120 V at D_{max} . The low-voltage-rated switch with low R_{DS-ON} can be selected for the reduction of conduction losses. Thus, the proposed converter is suitable for high-power applications as fuel cell systems in hybrid electric vehicles.

REFERENCES

- [1] W. Li, X. Lv, Y. Deng, J. Liu, and X. He, “A review of non-isolated high step-up DC/DC converters in renewable energy applications,” in *Proc. IEEE Appl. Power Electron. Conf. Expo.*, Feb. 2009, pp. 364–369.
- [2] W. Li and X. He, “Review of nonisolated high-step-up DC/DC converters in photovoltaic grid-connected applications,” *IEEE Trans. Ind. Electron.*, vol. 58, no. 4, pp. 1239–1250, Apr. 2011.
- [3] M. A. Laughton, “Fuel cells,” *IEE Eng. Sci. Edu. J.*, vol. 11, no. 1, pp. 7–16, Feb. 2002.
- [4] W. Jiang and B. Fahimi, “Active current sharing and source management in fuel cell-battery hybrid power system,” *IEEE Trans. Ind. Electron.*, vol. 57, no. 2, pp. 752–761, Feb. 2010.
- [5] P. Thounthong, S. Rael, and B. Davat, “Analysis of supercapacitor as second source based on fuel cell power generation,” *IEEE Trans. Ind. Electron.*, vol. 24, no. 1, pp. 247–255, Mar. 2009.
- [6] A. Khaligh and Z. Li, “Battery, ultracapacitor, fuel cell, and hybrid energy storage systems for electric, hybrid electric, fuel cell, and plug-in energy source applications: State of the art,” *IEEE Trans. Veh. Technol.*, vol. 59, no. 6, pp. 2806–2814, Jul. 2010.
- [7] L. Wang and H. Li, “Maximum fuel economy-oriented powermanagement design for a fuel cell vehicle using battery and ultracapacitor,” *IEEE Trans. Ind. Appl.*, vol. 46, no. 3, pp. 1011–1020, May/Jun. 2010.
- [8] M. Marchesoni and C. Vacca, “New DC–DC converter for energy storage system interfacing in fuel cell energy source applications,” *IEEE Trans. Power. Electron.*, vol. 22, no. 1, pp. 301–308, Jan. 2007.
- [9] G.-J. Su and L. Tang, “A reduced-part, triple-voltage DC-DC converter for EV/HEV power management,” *IEEE Trans. Power Electron.*, vol. 24, no. 10, pp. 2406–2410, Oct. 2009.
- [10] S. M. Dwari and L. Parsa, “A novel high efficiency high power interleaved coupled-inductor boost DC–DC converter for hybrid and fuel cell electric vehicle,” in *Proc. IEEE Veh. Power Propulsion Conf.*, Sep. 2007, pp. 399–404.

- [11] P. Xuwei and A. K. Rathore, "Novel interleaved bidirectional snubberless soft-switching current-fed full-bridge voltage doubler for fuel cell vehicles," *IEEE Trans. Power Electron.*, vol. 28, no. 12, pp. 5535–5546, Dec. 2013.
- [12] A. K. Rathore and U. R. Prasanna, "Analysis, design, and experimental results of novel snubberless bidirectional naturally clamped ZCS/ZVS current-fed half-bridge dc/dc converter for fuel cell vehicles," *IEEE Trans. Ind. Electron.*, vol. 60, no. 10, pp. 4482–4491, Oct. 2013.
- [13] O. Hegazy, J. Van Mierlo, and P. Lataire, "Analysis, modeling, and implementation of a multidevice interleaved dc/dc converter for fuel cell hybrid electric vehicles," *IEEE Trans. Power Electron.*, vol. 27, no. 11, pp. 4445–4458, Nov. 2012.
- [14] U. R. Prasanna, P. Xuwei, A. K. Rathore, and K. Rajashekara, "Propulsion system architecture and power conditioning topologies for fuel cell vehicles," in *Proc. IEEE Energy Convers. Congr. Expo.*, pp. 1385–1392.
- [15] Z. Zhang, Z. Ouyang, O. C. Thomsen, and M. A. E. Andersen, "Analysis and design of a bidirectional isolated dc–dc converter for fuel cells and supercapacitors hybrid system," *IEEE Trans. Power Electron.*, vol. 27, no. 2, pp. 848–859, Feb. 2012.
- [16] P. F. Ksiazek and M. Ordonez, "Swinging bus technique for ripple current elimination in fuel cell power conversion," *IEEE Trans. Power Electron.*, vol. 29, no. 1, pp. 170–178, Jan. 2014.
- [17] R. W. Erickson and D. Maksimovic, *Fundamentals of Power Electronics*, 2nd ed. New York, NY, USA: Springer, 2001.
- [18] A. I. Pressman, K. Billings, and T. Morey, *Switching Power Supply Design*, 3rd ed. New York, NY, USA: McGraw-Hill, 2009.
- [19] S. J. Finney, B. W. Williams, and T. C. Green, "RCD snubber revisited," *IEEE Trans. Ind. Appl.*, vol. 32, no. 1, pp. 155–160, Jan./Feb. 1996.
- [20] W. K. Thong and C. Pollock, "A novel low-cost RCD snubber for bifilar wound motors," *IEEE Trans. Ind. Appl.*, vol. 38, no. 3, pp. 688–694, May/Jun. 2002.
- [21] M. Serine, A. Saito, and H. Matsuo, "High efficiency DC/DC converter circuit using charge storage diode snubber," in *Proc. 29th Int. Telecommun. Energy Conf.*, 2007, pp. 355–361.
- [22] K. B. Park, G. W. Moon, and M. J. Youn, "Nonisolated high step-up stacked converter based on boost-integrated isolated converter," *IEEE Trans. Power Electron.*, vol. 26, no. 2, pp. 577–587, Feb. 2011.
- [23] H. Xiao and S. Xie, "A ZVS bidirectional DC–DC converter with phaseshift plus PWM control scheme," *Proc. Appl. Power Electron. Conf.*, vol. 23, no. 2, pp. 813–823, Mar. 2008.
- [24] P. Dos Santos, G. Giacomini, J. S. Scholtz, and M. Mezaroba, "Stepup/ step-down DCDC ZVS PWM converter with active clamping," *IEEE Trans. Ind. Electron.*, vol. 55, no. 10, pp. 3625–3643, 2008.
- [25] M. D. Seeman and S. R. Sanders, "Analysis and optimization of switched capacitor DC–DC converters," *IEEE Trans. Power Electron.*, vol. 23, no. 2, pp. 841–851, Mar. 2008.
- [26] F. L. Luo, "Six self-lift DC-DC converters, voltage lift technique," *IEEE Trans. Ind. Electron.*,